

Alblawi, Adel

## Article

# Fault diagnosis of an industrial gas turbine based on the thermodynamic model coupled with a multi feedforward artificial neural networks

Energy Reports

## Provided in Cooperation with:

Elsevier

*Suggested Citation:* Alblawi, Adel (2020) : Fault diagnosis of an industrial gas turbine based on the thermodynamic model coupled with a multi feedforward artificial neural networks, Energy Reports, ISSN 2352-4847, Elsevier, Amsterdam, Vol. 6, pp. 1083-1096, <https://doi.org/10.1016/j.egy.2020.04.029>

This Version is available at:

<https://hdl.handle.net/10419/244103>

### Standard-Nutzungsbedingungen:

Die Dokumente auf EconStor dürfen zu eigenen wissenschaftlichen Zwecken und zum Privatgebrauch gespeichert und kopiert werden.

Sie dürfen die Dokumente nicht für öffentliche oder kommerzielle Zwecke vervielfältigen, öffentlich ausstellen, öffentlich zugänglich machen, vertreiben oder anderweitig nutzen.

Sofern die Verfasser die Dokumente unter Open-Content-Lizenzen (insbesondere CC-Lizenzen) zur Verfügung gestellt haben sollten, gelten abweichend von diesen Nutzungsbedingungen die in der dort genannten Lizenz gewährten Nutzungsrechte.

### Terms of use:

*Documents in EconStor may be saved and copied for your personal and scholarly purposes.*

*You are not to copy documents for public or commercial purposes, to exhibit the documents publicly, to make them publicly available on the internet, or to distribute or otherwise use the documents in public.*

*If the documents have been made available under an Open Content Licence (especially Creative Commons Licences), you may exercise further usage rights as specified in the indicated licence.*



<https://creativecommons.org/licenses/by-nc-nd/4.0/>



## Research paper

# Fault diagnosis of an industrial gas turbine based on the thermodynamic model coupled with a multi feedforward artificial neural networks

Adel Alblawi

Mechanical Engineering Department, College of Engineering, Shaqra University, Dawadmi, P.O. 11911, Ar Riyadh, Saudi Arabia

## ARTICLE INFO

## Article history:

Received 31 January 2020  
 Received in revised form 25 March 2020  
 Accepted 19 April 2020  
 Available online xxxx

## Keywords:

Energy efficiency  
 Multi feedforward artificial neural network  
 Industrial gas turbine  
 Engine performance and deterioration  
 Thermodynamic model  
 Fault diagnosis

## ABSTRACT

In the study presented in this paper, the deterioration in the performance of an industrial gas turbine during the operation design point was simulated by using the thermodynamic principle and a multi feedforward artificial neural networks (MFANN) system. Initially the thermodynamic model was constructed using the components performance map technique, that entailed calculating the operating point which was compliant with the performance map for each component. The various design operation points were generated by changing the engine component's efficiency or outer environmental conditions and simulating the engine's performance for each case. The MFANN model was constructed by using these operation points for the training and testing stage. In this way, the two MFANN models were established. The aim of the first model was to calculate the engine's performance while the second model was used to detect the deterioration of the components of the engine. This paper presents a robust fault diagnosis system for gas turbine degradation detection with the aim of improving energy efficiency.

© 2020 The Author. Published by Elsevier Ltd. This is an open access article under the CC BY license (<http://creativecommons.org/licenses/by/4.0/>).

## 1. Introduction

A gas turbine engine is a thermodynamic machine that performs its functions efficiently without exceeding the design limitations. It uses fuel and air to convert the chemical power of the fuel into mechanical power, such that the air and gas (products of combustion) are working fluids in cold and hot sections, respectively (Talaat et al., 2018).

Gas turbine engines are used in industrial and aerospace applications. In industrial applications, gas turbine engines are widely used to produce mechanical power for:

- driving various loads such as large pumps and compressors,
- driving tanks, marines and transportation vehicles, and
- driving generators for electrical power production.

Gas turbines may be used in electrical power plants alone or in combination with a steam turbine, whether in combined cycles, or in cogeneration for both electrical power and industrial heat treatment. The combined cycle power plant, commonly used for power generation, is featured with one or more gas turbines and often one steam turbine to offer high efficiency (Talaat et al., 2018).

The performance of a gas turbine depends on several factors, including external factors which are difficult to control. Examples are surrounding environmental pollution, and increased air temperature and humidity. Other factors that can be repaired are fouling in the compressor and the turbine which may be repaired by the washing of these components. Erosion occurring in the components is repaired by replacing the defective part (Talaat et al., 2018; Cohen et al., 1987; Norvaisis, 1974; Gobran, 2013).

The continuing operation of an engine leads to the occurrence of the above-mentioned factors. However, one can delay these occurrences through the safe operation of the engine, the use of better-quality fuels and with regular maintenance. Many researchers have dealt with this issue by using the principles of thermodynamics to build representational models of the degradation affecting gas turbine performance. These thermodynamic models are used to represent the engine components by the application of performance maps. The performance maps simulate the deterioration with modification of the compressor and turbine performance (Talaat et al., 2018; Lakshminarasimha et al., 1994; Roumeliotis, 2010). The thermodynamic models are utilized to calculate changes in the gas turbine performance if deterioration exists in the engine components. Accordingly, the researchers proposed to use an artificial intelligence network in order to detect and then predict the deterioration in a gas turbine (Talaat et al., 2018; Syverud, 2007; Ogbonnaya, 2011).

J. Bai et al. proposed an identification method for parameter uncertain linear model for an aero gas turbine (GT) (Bai et al.,

E-mail address: [aalblawi@su.edu.sa](mailto:aalblawi@su.edu.sa).

2019). This was performed by using nonlinear programming. Through this method, the turbine model identification problem was solved by means of considering the model parameter uncertainty. The model, designed for the fault diagnosis (FD) and engine control of the GT, could simulate the real state of the engine within a 1% error range.

S. Amirkhani et al. proposed a robust FD as an uncertain nonlinear system using a new adaptive threshold method (Amirkhani et al., 2019). This method was proposed for a power plant GT. They employed the Monte Carlo simulation approach to determine the bounds of the adaptive threshold and to identify the Neural network thresholds modelling. The proposed model was found to achieve robust, accurate and reliable performance without any assumptions regarding the nonlinearity type.

P. K. Wong et al. proposed a novel application for extreme learning machine (ELM) algorithm for building a real time FD system (Wong et al., 2014). The data preprocessing techniques are integrated in this proposed system. Wavelet packet transform and time-domain statistical features are proposed for getting the vibration signal features. Kernel principal component analysis is then applied to reduce the redundant features in order to shorten the fault identification period and improve accuracy. In order to evaluate the performance of the proposed model, a comparison between the support vector machines (SVM) and the ELM algorithms was performed upon experimental data. While each algorithm provides comparable accuracy, the time of fault identification using the ELM was extremely short compared to that of the SVM.

In 2020, J. Li and Y. Ying proposed a novel gas path (GP) diagnostic method (Li and Ying, 2020). This was performed through three steps. The first was proposing an equivalent cooling flow processing method for thermodynamics modelling of the GP diagnostic. Then, they proposed a steady state diagnostic scheme under transient conditions based on local optimization algorithm. Afterwards, the diagnostic performance was compared using two local optimization algorithms of Newton–Raphson and Kalman filters. The case studies used, proved that the proposed model is effective in detecting both component gradual failure and abrupt fault quantitatively. Moreover, it was found that the diagnostic method based on Newton–Raphson algorithm has better real-time performance than the Kalman filter algorithm.

S. Zhong et al. proposed a new gas turbine fault diagnosis based on conventional neural network (CNN) training (Zhong et al., 2019). It is well known that the CNN is effective for determining errors in larger size training data sets. Consequently, it is presupposed that this prevents the application of the CNN from accurately diagnosing errors in smaller sized training data sets. However, in their research, the authors used the CNN to determine errors in smaller size training data. They utilized a feature mapping method to extract the feature representations from the normal training data set by reusing the internal layers of the CNN trained on the normal dataset. Consequently, the researchers have determined the efficacy of the CNN to diagnose errors in both large and smaller sized training data sets.

H. Hanachi et al. suggested a new fault detection method for gas turbines based on a hybrid diagnostic framework that integrates the results from a measurement-based fault parameter with a fault propagation model (Hanachi et al., 2019). The hybrid framework used a novel particle filter (PF) structure with redundant measurements. This technique simplifies updating the particle weights while reducing the dimensionality of the measurement likelihood. This framework was applied on GT gas-path data with four different gradually worsening faults. The results showed that the diagnostic accuracy displayed an almost ten-fold increase compared to the accuracy of the previous fault parameter estimation scheme.

Kazemi and Yazdizadeh presented a new scheme for fault diagnosis and isolation (FDI) including inversion-based fault reconstruction and optimal state observers (Kazemi and Yazdizadeh, 2020). The optimal state observers concern a class of nonlinear systems, subject to concurrent faults and unknown disturbances that represent the nonlinear dynamic model of a GT. The original system was transformed into a new form in which both observers were applied for fault diagnosis for each fault type through coordinate transformation. The coordinate transformation came from observability concepts in differential geometry. The presented approaches were applied for the FDI of a gas turbine model subject to compressor efficiency, compressor mass flow capacity, and actuator faults, in addition to an unknown disturbance. The simulation results proved that the proposed FDI schemes were a good tool for the GT diagnostics.

D. Zhou et al. proposed a method for a gas path fault diagnostic for the GT based on the changes in the blade profiles (Zhou et al., 2020). They used the blade profile change parameters to replace the traditional performance degradation parameters to achieve the gas path fault diagnosis. The deterioration of the GP was characterized by the blade profile change parameters, including the blade thickness increment and blade roughness. In addition, the velocity, temperature, and pressure fields were numerically obtained. The results proved the effectiveness of the proposed diagnostic model in GP fault detection.

A. Guasch et al. proposed two different approaches for improving the FD of GT based on the embedded information in the control system (Guasch et al., 2000). The first system suggests an automatic development for the trouble shooting of the deterministic knowledge embedded within the Programmable Logic Controller (PLC). This system attempts to overcome the difficulties of the FD especially for the old GTs. The second approach is based on the analysis of the digital control system which detects the faults in the feedback systems.

Simani and Patton proposed a procedure based on a model for FDI of faults on a gas turbine simulated process (Simani and Patton, 2008). The main objective presented an identification scheme in connection with dynamic observer or filter design procedures for diagnostic purposes. Large numbers of simulations of the test-bed process and Monte Carlo analysis were used for assessing experimentally the capabilities of the developed FDI scheme.

In the gas turbine diagnosis field, the artificial neural network (ANN) may be more effective relative to other artificial intelligence systems. In the degradation cases, it is difficult to use the mathematical models to describe the behaviour of the system. However, the ANN uses training data to judge the behaviour of the system upon the introduced behaviour. Subsequently, it is expected to give more trusted results as it simulates the actual behaviour of the system during the degradation (Talaat et al., 2018). The new techniques of the artificial neural networks, such as the multi feedforward artificial neural network (MFANN) can be utilized for diagnosing different faults of industrial gas turbines. The MFANN has the ability of system modelling. It enables the monitoring of an enormous group of different and connected inputs and outputs that employs the concept of ANN non-linear relationships with high accuracy (Talaat et al., 2018; Bettocchi et al., 2002).

The disadvantages of ANNs are that they may generate error in the forecasting process. In addition, training may be unstable, and many parameters need to be determined. Small sample size and low convergence issues are two common drawbacks of ANNs. A neural network model is constructed by choosing the input data and output data (Farahat and Talaat, 2012; Talaat et al., 2020, 2019).

Consequently, the MFANN has the advantage of overcoming the disadvantages of ANNs by

- using the concept of the forward and non-linear algorithm of the network, and
- the different weights and special structure of the network.

The only difficulty in the MFANN technique is the suggested numbers of neurons and hidden layers. These number of neurons and number of hidden layers should be carefully selected in the MFANN because they affect the accuracy of training. With these selections in place, the MFANN becomes more suitable than the classical modelling of ANN techniques (Asgari et al., 2013).

The treatment of different input measurement layers and the required output are usually completed using a suitable number of neurons in the hidden layers for the training stage. Often the selection process involves training of the network several times with a different neuron number and then concluding the selection process with the appropriate neuron number. Though these hidden layers are impalpable for the users of these networks, they have a major effect on the overall result (Farahat and Talaat, 2012; Tamuno-ojuemi Ogaji, 2003).

Degradation in the industrial gas turbine is due to the deterioration factors that surround the engine. Due to an increase in fuel consumption, these factors lead to high operational costs. The independence of the electricity market promotes competition between the objective of the electrical power investor and responsibility towards a cleaner environment. Because of the high cost of fuel, the plant operators must be concerned with detecting all forms of gas turbine performance deterioration wherever they occur. With a significant increase in the price of fuel, the diagnosis of degradation becomes of vital importance to maintain a healthy and optimal operational performance of the industrial gas turbine. Often a mathematical model is designed to generate the degradation database because of the difficulty in obtaining this information from the real engine. The Mathematical model is then determined as the detection tool that is used to analyse the engine measurement data by means of the database created by it.

The deterioration factors that can affect the performance of a gas turbine are many. In the study presented in this paper, some of these factors had a more noticeable effect than others on the overall performance of the gas turbine in the study. They were as follows: the combustion efficiency, compressor efficiency, turbine efficiency, air capacity efficiency, and air filter efficiency. Other degradation factors that can affect the performance are the faults in intake and outtake ducts, air and gas leakages, and guide vanes mistaking. In this present study some experimental data were that were used are as follows: pressure ratio, air flow rate, fuel flow rate, compressor discharge temperature, turbine inlet temperature, relative speed and power load. The rest of the parameters were: working fluid flow rate and components efficiency which were calculated using the thermodynamic model with iterations to validate the mass and energy balances in the deterioration cases. This data was used to train and test the proposed MFANN model.

## 2. Thermodynamic proposed model

In this study, the thermodynamic model was constructed (by using MATLAB program) for the calculation of the steady state performance of a single spool gas turbine GE-9EA, simple Brayton cycle during both start-up (64% to 100% design speed) and loading (100% design speed).

To overcome the lack of the real engine component characteristics, alternative maps were built by applying suitable scaling techniques to the available real maps.

Fig. 1 represents the model of the thermodynamic simple process cycle of industrial turbine, and these processes are explained as follows:

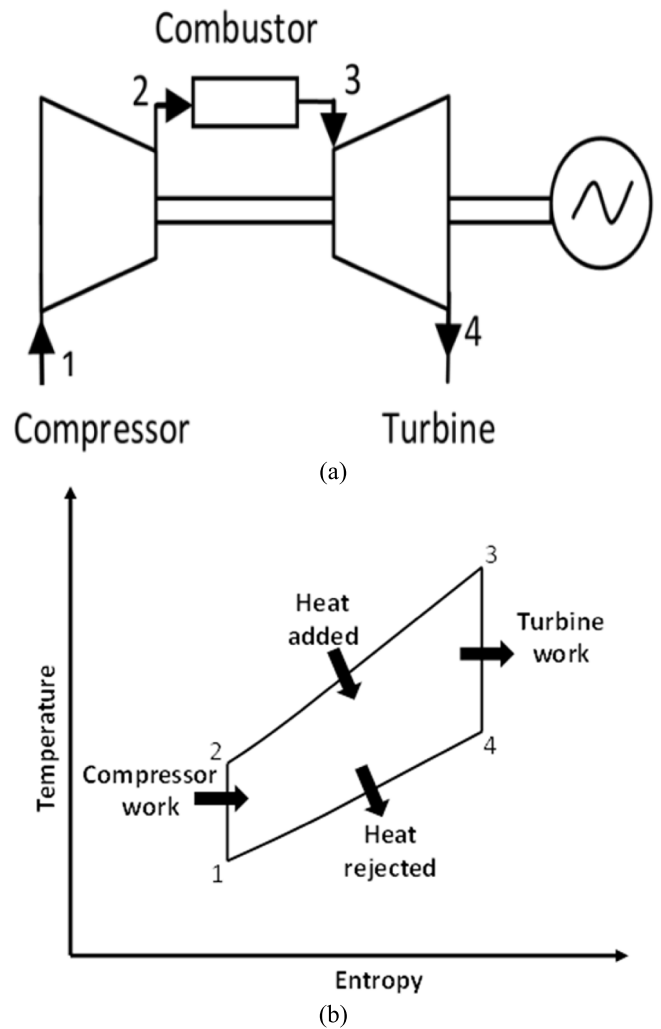


Fig. 1. (a) Schematic diagram of a simple industrial turbine; (b) Thermodynamic simple process cycle of an industrial turbine.

- from 1 to 2 which represents the air compressed in the compressor part,
- from 2 to 3 which the burning of fuel in the part of the combustion chamber, and
- from 3 to 4 which represents the part required to produce the output electrical power by the expanding process.

The target of this model was to find the suitable operating point and properties of the compressor and turbine by considering the mass flow rate, engine temperature, engine efficiency and pressure for all available operating points.

The model was considered under the following assumptions:

1. The main operating points of the cycle appeared in Fig. 1(a) were considered including the filter before point No. 1.
2. The last point considered was the turbine exit.
3. The connections and casings of both the compressor and the turbine had no leakages or bleeds.

The thermodynamic process considering the process from 1 to 2 or from 3 to 4, was governed by the following relations (Talaat et al., 2018).

$$T_{(i+1)s} = T_i * (\pi_{i : (i+1)})^{\pm(\frac{\gamma-1}{\gamma})} \quad (1)$$

**Table 1**  
Deterioration domain of engine components.

Component degradation	Ideal case	Max deterioration	Case 1	Case 2	Case 3	Case 4	Case 5
Compressor efficiency ( $\eta_c$ ) deterioration %	0.814 (or 0%)	0.06↓ (.765) or (100%)	0.02↓ or 33.3%	0.04↓ or 66.6%	0.06↓ or 100%	0.02↓ or 33.3%	0.06↓ or 100%
Turbine efficiency ( $\eta_t$ ) deterioration %	0.821 (or 0%)	0.04↓ (.788) or (100%)	0.01↓ or 25%	0.02↓ or 50%	0.04↓ or 100%	0.02↓ or 50%	0.01↓ or 25%
Flow capacity efficiency ( $\eta_{flow}$ ) deterioration %	1.0 (or 0%)	0.06↓ (.94) or (100%)	0.03↓ or 50%	0.06↓ or 100%	0.03↓ or 50%	0.03↓ or 50%	0.06↓ or 100%
Combustion efficiency ( $\eta_{c.c}$ ) deterioration %	0.92 (or 0%)	0.06↓ (.864) or (100%)	0.06↓ or 100%	0.03↓ or 50%	0.03↓ or 50%	0.06↓ or 100%	0.03↓ or 50%

where,  $T_i$ ,  $T_{(i+1)s}$ ,  $\pi_{1:(i+1)}$  are the inlet temperature, the isentropic discharge temperature and the pressure ratio of compressor or turbine respectively,  $\gamma$ : is the isentropic index, for process from 1 – 2 ( $i = 1\&+$ ) and for process from 3 – 4 ( $i = 3\&-$ ).

$$T_{(i+1)cs} = T_{(i+1)s} * e^{\pm\left(\frac{s_i - s_{(i+1)}}{R}\right)} \quad (2)$$

where,  $T_{(i+1)cs}$ : is the corrected isentropic discharge temperature of compressor or turbine,  $s$ : represents the entropy and  $R$ : represents the gas constant.

$$\begin{cases} h_{(i+1)} = h_i + \frac{(h_{(i+1)cs} - h_i)}{\eta_c} \\ \text{or} \\ h_{(i+1)} = h_i + \frac{(h_{(i+1)cs} - h_i)}{\eta_t^{-1}} \end{cases} \quad (3)$$

where,  $h$ : represents the enthalpy,  $\eta_c$ : is the compressor efficiency and  $\eta_t$ : is the turbine efficiency. The values of  $h$  and  $s$  can be obtained as functions of compressor temperature as given by (Talaat et al., 2018; McBride et al., 2002).

$$\frac{h(t)}{R} = -a_1 T^{-1} + a_2 \ln(T) + a_3 T + \frac{a_4}{2} T^2 + \frac{a_5}{3} T^3 + \frac{a_6}{4} T^4 + \frac{a_7}{5} T^5 + b1 \quad (4)$$

$$\frac{s(t)}{R} = -\frac{a_1}{2} T^{-2} - a_1 T^{-1} + a_3 \ln(T) + a_4 T + \frac{a_5}{2} T^2 + \frac{a_6}{3} T^3 + \frac{a_7}{4} T^4 + b2 \quad (5)$$

Using the  $h_2$  by inverse to get  $T_2$ , Eq. (6) represent the energy balance

$$m_a^* * h_2 + \eta_b * m_f^* * HV = (m_a^* + m_f^*) * h_3 \quad (6)$$

where, the  $m_a^*$ : is the compressor flow rate,  $m_f^*$ : is the fuel flow rate, HV: heating value and  $\eta_b$ : is the combustion efficiency. So, by assuming that, the  $T_3$ (turbine inlet temperature) then, the  $m_f^*$  has been calculated.

### 2.1. Engine main components degradation simulated

The main engine components were the axial compressor, combustion chamber and axial turbine. The degradation of these engine components represented the reducing of efficiency and mass flow rate of each component. When degradation occurred on the proposed model, the modify factors were used to identify the extent of engine component deterioration. The modify factor (M.F) for this component is represented by the following relation (Talaat et al., 2018; Roumeliotis, 2010).

$$M.F = \frac{X_{degrade}}{X_{ideal}} \quad (7)$$

where,  $X_{degrade}$  and  $X_{ideal}$  are the engine component parameters with degradation and ideal case respectively.

Specifically, for compressors and turbines, the degradation has been represented by using two modify factors. The first factor represents the component flow rate capacitance, and the second represents the component efficiency.

The component flow rate capacitance factor is:

$$M.F_m = \frac{m^*_{degrade}}{m^*_{ideal}} \quad (8)$$

The component efficiency factor is:

$$M.F_\eta = \frac{\eta_{degrade}}{\eta_{ideal}} \quad (9)$$

where,  $m^*$ : represents the mass flow rate component and  $\eta$ : represents the efficiency component.

From previous equations, the industrial turbine thermodynamic map was modified by using the new modifying factors (mass flow rate and efficiency), and for the combustion section, the degradation was represented by the efficiency factors ( $\eta_{c.c}$ ).

### 2.2. Degradation data generation

The deterioration of the engine was represented by the degradation of one or more of the engine's components, so assessing the probability of various deterioration cases of the components, together with identifying the surrounding environmental conditions and the air inlet system state was important. Table 1 illustrates the deterioration domain of engine components. The analysis was applied to design point (full load) and conditions of ambient temperature range between 288 and 308 K. These variations of the ambient temperature were recorded at each case to be used in the thermodynamic model considered as it affected the operation of the compressor and hence affects the operation of the cycle.

The turbine output temperature was estimated to be constant during the simulation. This simulation generated 4788 fault data points. 4095 cases for non-repeated combinations of 12 objects, calculated by the function of ( $2^n - 1 = 2^{12} - 1 = 4095$ ), 592 data cases were considered multi faults based on real measured data and 101 data points were used for testing the model.

### 2.3. Proposed model matching procedure

At the design point, assumptions were made of four variables in order to find the optimal operating point on the industrial turbine map. Thus, four matching constraints had to be satisfied, see Fig. 2.

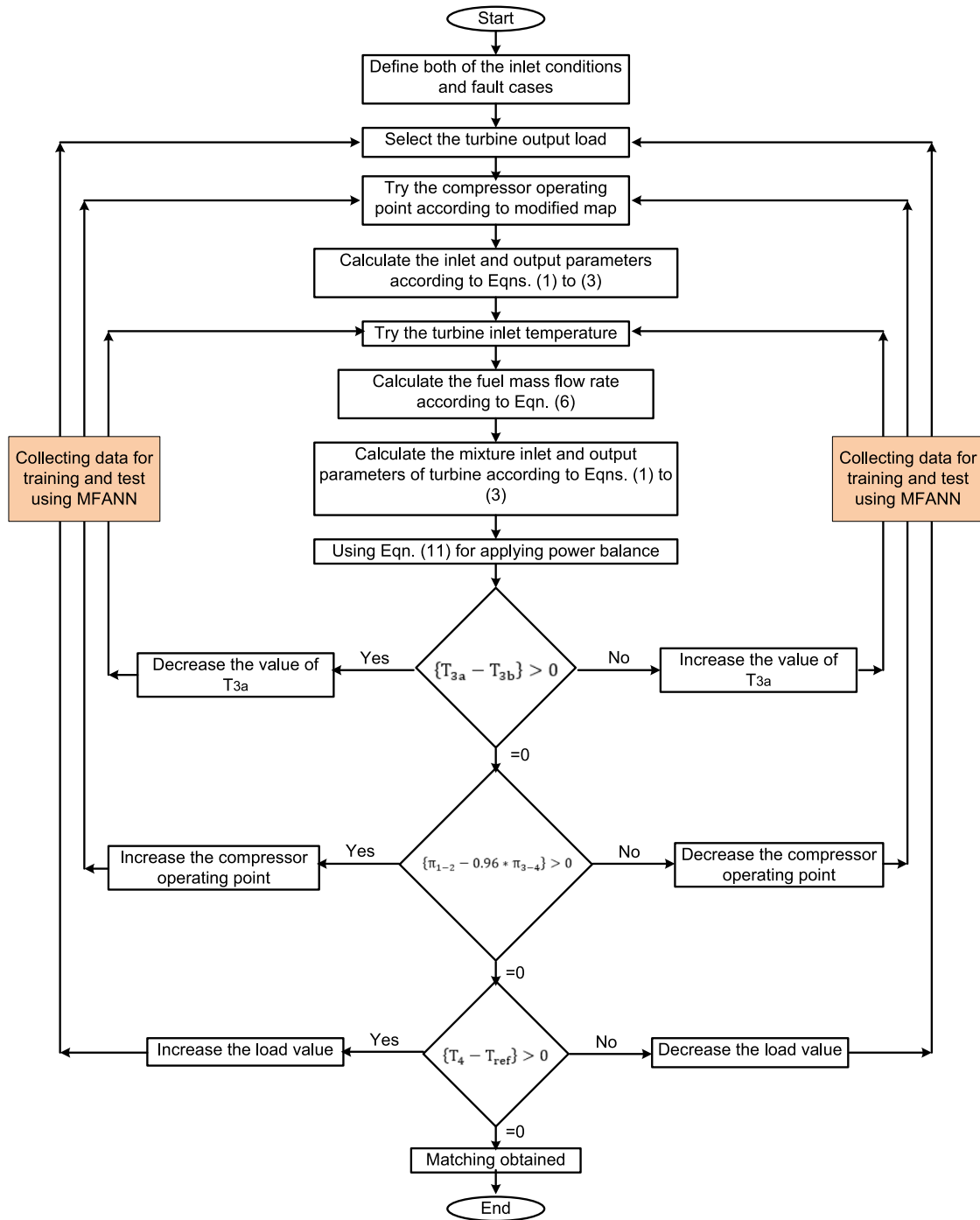


Fig. 2. The proposed model matching procedure.

2.3.1. The continuity of mass flow rate between compressor and turbine

$$m_t = m_c + m_f \tag{10}$$

where,  $m_t$ ,  $m_c$  and  $m_f$  are the mass flow rate of turbine, compressor and fuel respectively.

2.3.2. The generated power resulting from compressor and turbine power

$$\text{load} = P_t - P_c \tag{11}$$

where, load: represents the generated power, and  $P_t$  and  $P_c$  are the power from turbine and compressor respectively.

2.3.3. Generator nominal frequency 50 Hz or 3000 rpm

$$N_t = N_c = 3000 \text{ rpm} \tag{12}$$

where,  $N_t$  and  $N_c$  are the rotational speed of turbine and compressor respectively.

Assume combustion chamber pressure loss equal to  $0.04 \times$  Compressor pressure so,  $\pi_{1-2} = 0.96 * \pi_{3-4}$

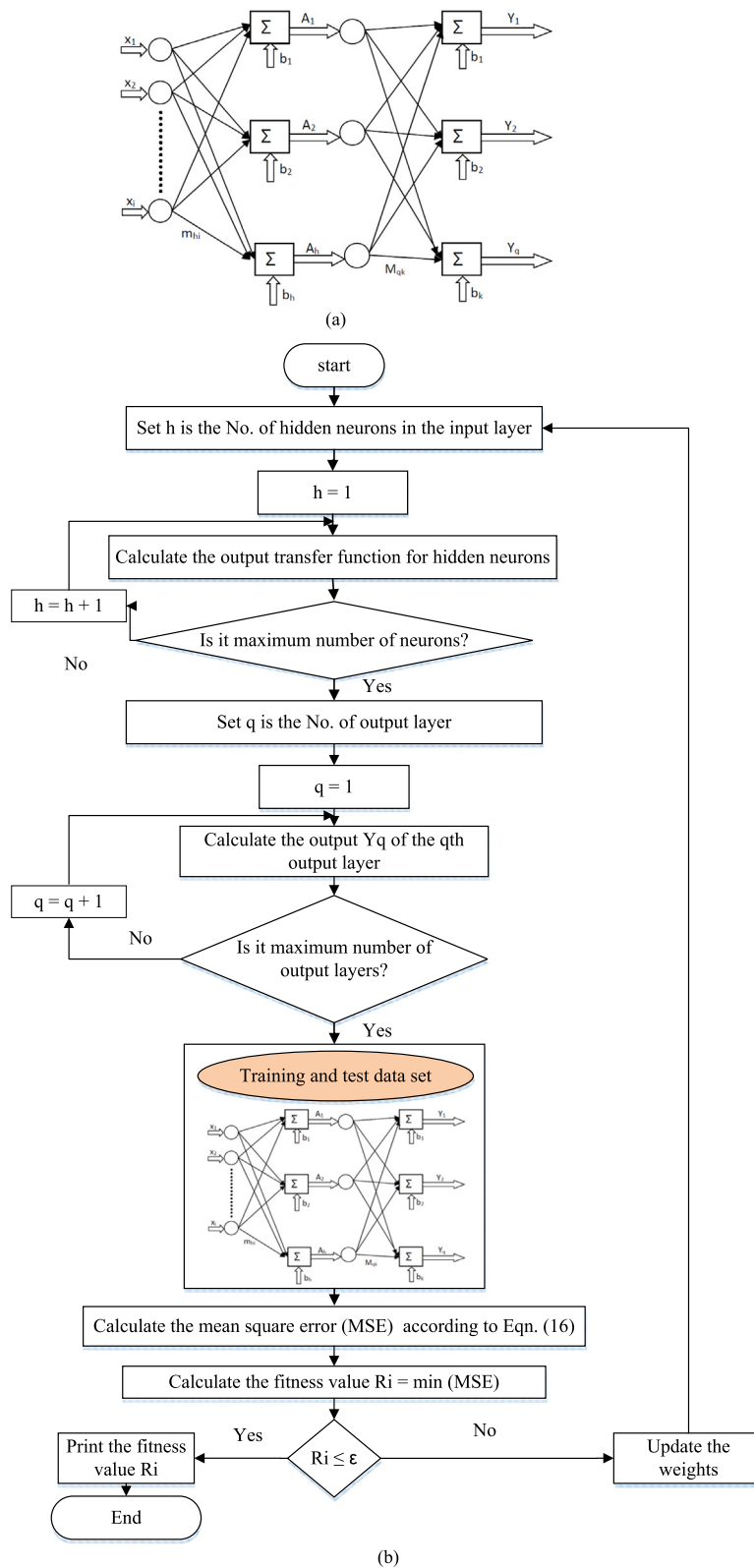


Fig. 3. Training Algorithm of MFANN, (a) MFANN activation function and hidden layer of neurons, (b) MFANN training methodology.

2.3.4. The temperature limited

$$T_4 = T_{ref} = 838 \text{ K} \tag{13}$$

where,  $T_4$  and  $T_{ref}$  are the output temperature of turbine and control limit temperature respectively.

3. Proposed technique of MFANN

ANN training depended on multi-inputs or multi-outputs. The least mean square (LMS) was used to train the multi-inputs that is called MFANN while a back propagation artificial neural network was used in case of multi-outputs training (Talaat et al., 2018,

2020). The MFANN was used because it enhances the performance and reduces the training time. In addition, the MFANN is considered simple and convenient to most of the nonlinear and complex problems with large number of inputs.

In the MFANN-based forecasting fault system diagnosis, a MFANN with one hidden layer was used in this study. The input layer had several neurons equal to the number of network inputs, the hidden layer had N neurons and the output layer had M neurons. The data was classified into three types in the MFANN (training, testing and validation data set). The output of the MFANN was the forecasted fault system diagnosis in the case of fault detection or the efficiency performance in the case of degradation detection. The transfer function for the hidden neurons was the log-sigmoid transfer function (Talaat et al., 2020), and the out-put transfer function was a linear activation function. Fig. 3 illustrates the algorithm process for training the MFANN.

The output of the *h*th hidden neuron is calculated by:

$$A_h = \sum_{i=1}^N f [(x_i \times m_{hi}) + b_h] \quad (14)$$

where,  $m_{hi}$  is the weights between the *i*th input neuron and *h*th hidden neuron,  $b_h$  is the base of the hidden layer neuron,  $x_i$  is the *i*th input,  $A_h$  is the output of the hidden layer, see Fig. 3.

The output  $out_q$  layer is determined by:

$$Y_q = \sum_{k=1}^M (M_{qk}A_h) + b_k \quad (15)$$

where,  $M_{qk}$  is the weights between the *i*th and the *q*th output neurons.

To obtain the training algorithm performance, the error was determined by finding the difference between MFANN output and the target output.

Where,  $Y_m$  is the input to the system as training and check data,  $Y$  is the output target which represents the prediction of the system degradation, *i* is the number of data sets and *N* is the number of training patterns. Hence, the Mean Square Error (MSE) is defined according to Eq. (16) as given by (Talaat et al., 2018; Farahat and Talaat, 2012; Talaat et al., 2020),

$$MSE = \frac{1}{N} \sum_{i=1}^N \left\{ \frac{Y_{mi} - Y_i}{Y_{mi}} \right\}^2 \quad (16)$$

The fitness value of the training pattern is computed by:

$$Fitness (R_i) = \min(MSE) \quad (17)$$

#### 4. MFANN model for industrial turbine performance calculated

The function of MFANN model was similar to that of the thermodynamic model, but the MFANN model was better for the computation of time, because thermodynamic models carry out different degrees of iterations of nonlinear equations, which takes a long time relative to those performed by the MFANN. Moreover, the MFANN was able to find errors in the operating points, which is difficult to determine in thermodynamic models especially in cases of multiple faults applications.

The required data for constructing the MFANN model was generated in the available operating range of the engine using the thermodynamic model. About 4788 data sets was employed for the training of an accurate MFANN-based model for the identified engine performance. The MFANN was used and accommodated the degree of degradation of the four components with the corresponding air inlet temperature and local air filter loss coefficient

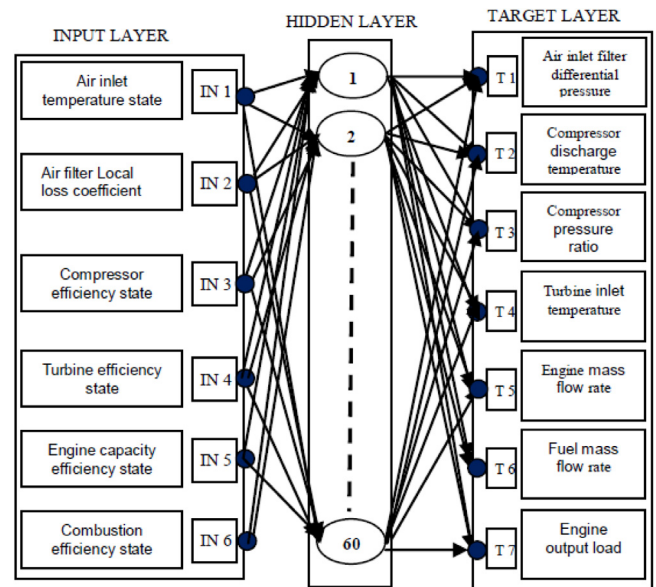


Fig. 4. MFANN industrial turbine performance model structure.

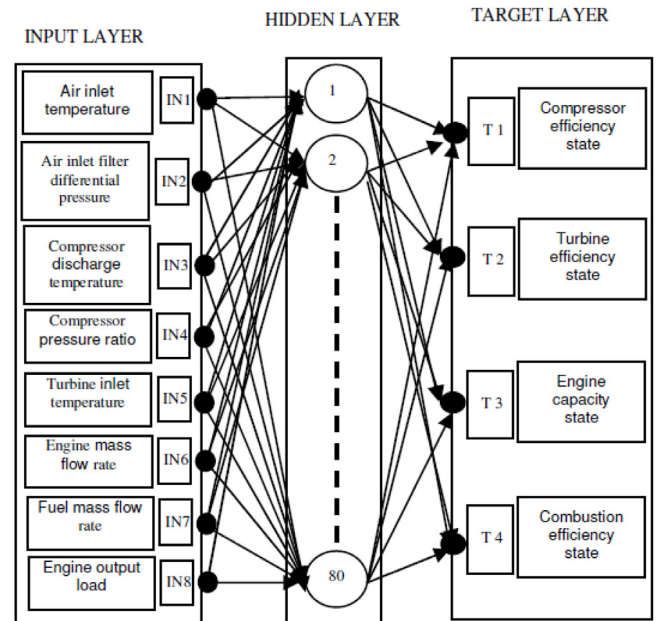


Fig. 5. MFANN model for industrial gas turbine degradation detection.

for input. For output, the other seven measurements were used. This data was utilized for the training and testing of the MFANN while choosing the optimal structure – the number of hidden layers, number of neurons, type of transfer function – that satisfied the minimum mean squared error. Fig. 4 shows the structure of the MFANN industrial turbine performance model, which was integrated from one hidden layer – sixty neurons of this hidden layer – and an employed log-sigmoid transfer function.

#### 5. MFANN model for industrial gas turbine degradation detection

Performance degradation in industrial gas turbine was used to predict the engine component condition (efficiency and flow capacity) for a given performance parameter. The MFANN model



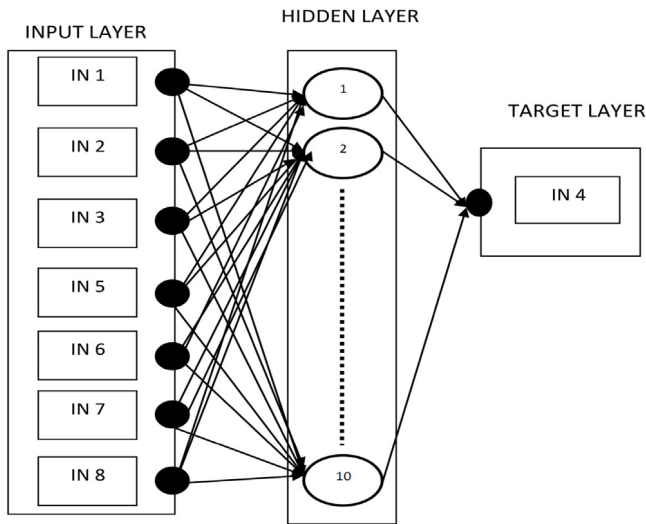


Fig. 6. Example of analytic MFANN models for the fourth input.

The MFANN input selection was proportional to the measurement sensors that were available in the real engine, and therefore, the output represented the degradation percentage of each engine component. The eight measurements represented the MFANN input and the four components degradation degree represented the MFANN output. The best MFANN structure was based on the training and testing data considering the optimal values of number of neurones and hidden layers with suitable transfer function.

Fig. 5 shows structure of the MFANN model for industrial gas turbine degradation detection, which was integrated from one hidden layer, eighty neurones of this hidden layer and used logistic transfer.

5.1. Input layer analysis system for the MFANN degradation detection model

The accuracy of the MFANN model's performance depended on the input data. Therefore, any imbalance in input could lead to failure in the degradation detected. This proposal offers an alternative solution to complete the degradation detected in the case of a defect in only one element in the input layer. Each element was compared with a maximum and minimum value to determine the input elements defect.

The analysis system usually does not work in the case of a defect in more than one of the input elements, or if the value of any of the elements is greater than or less than the maximum and

was developed to calculate the engine component characteristic parameters when measurements were available. All the data used to train and test MFANN is taken from the thermodynamic model.

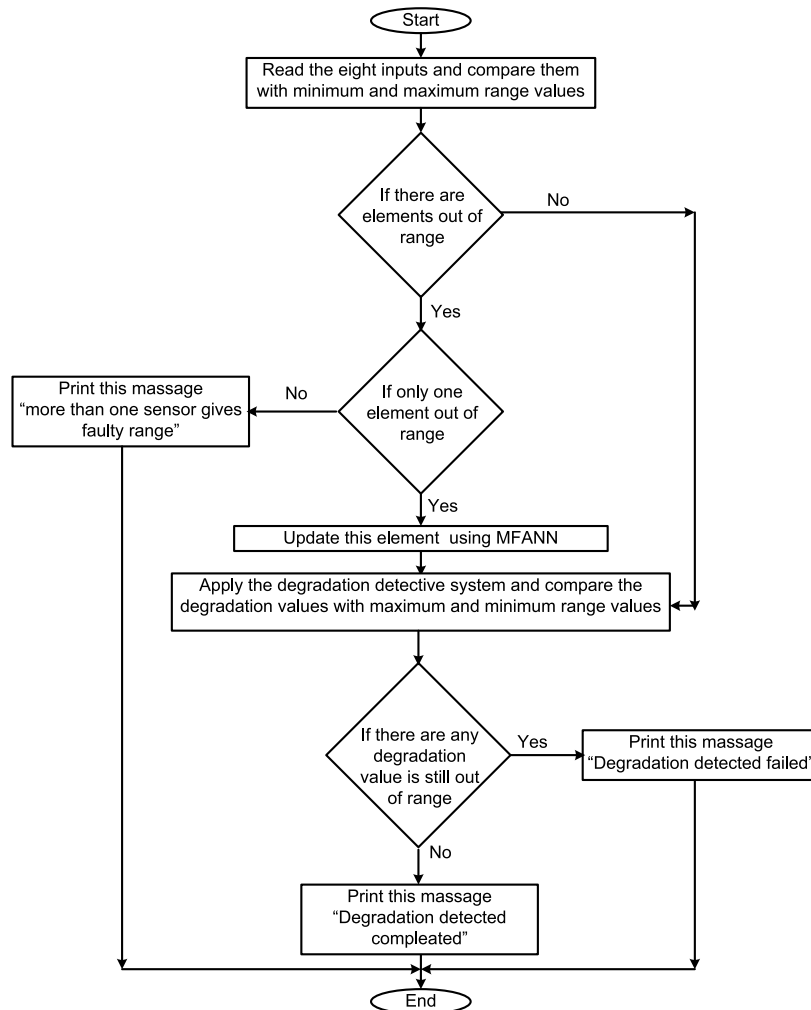


Fig. 7. Flowchart for integrated degradation detected system.

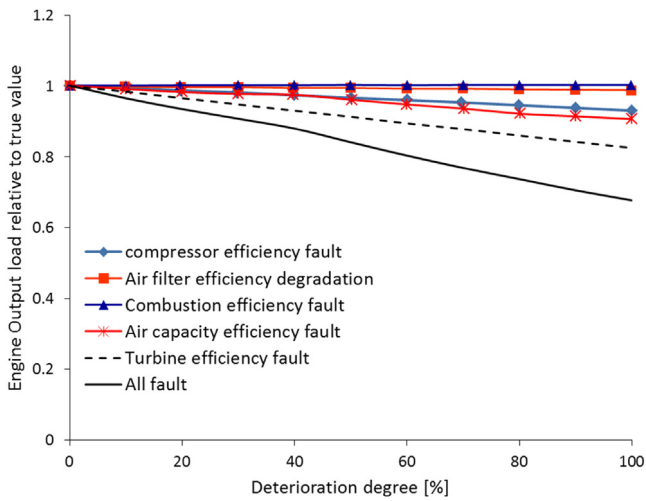


Fig. 8. The variation of engine output power with increased by deterioration degree.

the minimum value, respectively. The MFANN used to build this system was constructed to include a MFANN model for each input element, thus the target for the MFANN model was one element while the other seven inputs remained constant.

5.2. Analytic MFANN detection model

Fig. 6 shows an example of analytic MFANN models for the fourth input element (pressure ratio), which was integrated from one hidden layer, twenty neurons of this hidden layer and used logistic transfer.

In this way, the eight MFANN models were developed. These models were tested with all training data (about 4059 cases) which gave accurate results with an accepted percentage error.

These eight MFANN models were merged with the degradation detected MFANN model to construct an integrated system for industrial gas turbine engine degradation detection.

Fig. 7 illustrates the procedure flow chart for degradation detected by input measurement analysis. This figure indicates the flow chart for the degradation detection using the MFANN model with eight sensor data inputs as shown in Fig. 5. Based on this

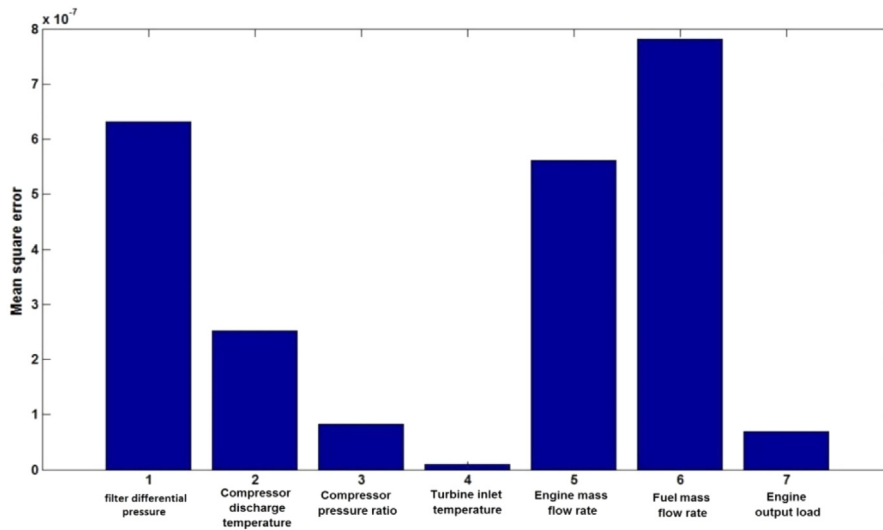


Fig. 9. MSE between thermodynamic model and MFANN performance model.

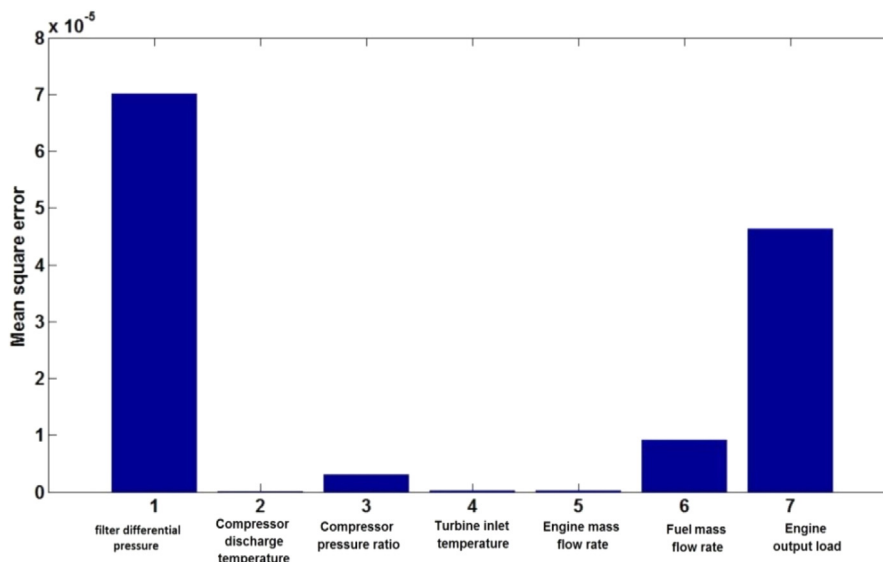


Fig. 10. MSE between thermodynamic model and MFANN degradation detection model.

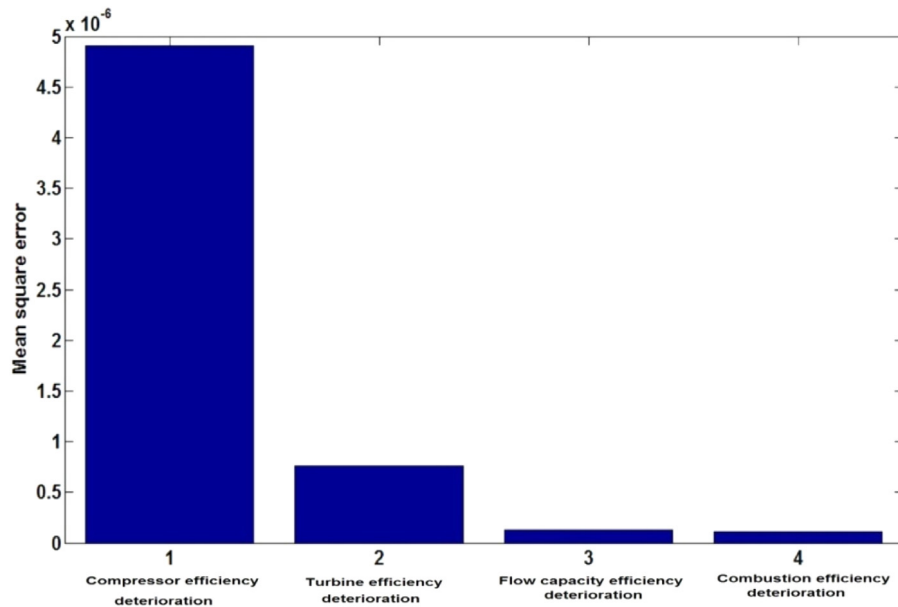


Fig. 11. MSE between engine model and degradation detection system (Air inlet temperature = 0).

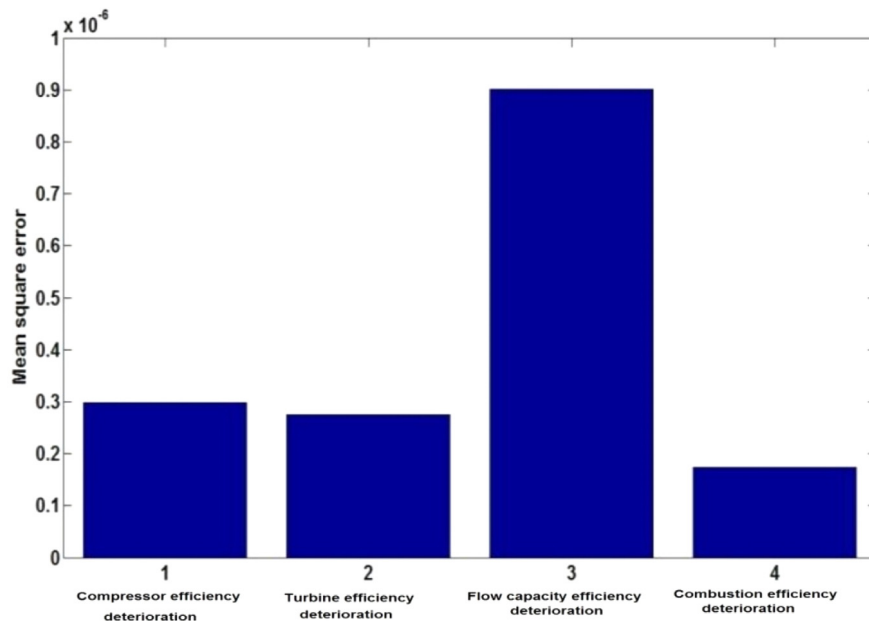


Fig. 12. MSE between engine model and degradation detection system (at Air inlet filter differential pressure = 0).

data, the MFANN model detected the fault case. Then, it applied the degradation upon the detected fault, detected the solution for this specific fault and stored this information for this solution. If the applied solution detected out of range data, it displayed the following message: “degradation detection failed”.

## 6. Testing of MFANN models

The testing data was generated by using the thermodynamic model. During the duration of the training phase of the MFANN models, the testing data was evaluated to 101 samples whenever data was not in use. The results were as follows:

- The MFANN performance model was tested firstly by entering the engine component's degradation conditions and then by comparing the MFANN results with the existing test

results from the real readings and finally by comparing the measurement results with the corresponding testing data measurements.

- The MFANN degradation detection model was tested by entering the engine's measurement parameters and by comparing the MFANN results with the corresponding degradation detected conditions in testing data.
- The integrated degradation diagnosis system was tested by entering the eight measurement parameters and by forcing the zero value to any one of them and then comparing the output results of the system with the testing results.

This process was repeated for each individual element of measurement.

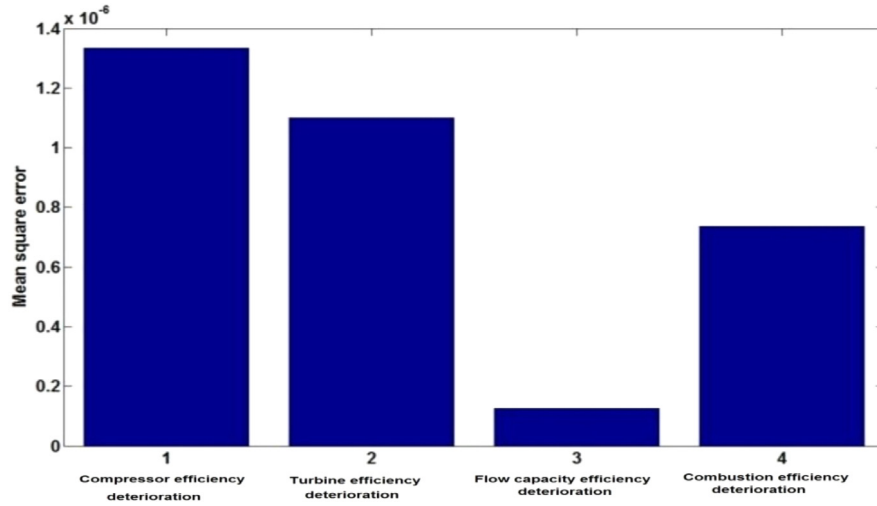


Fig. 13. MSE between engine model and degradation detection system (at Compressor discharge temperature = 0).

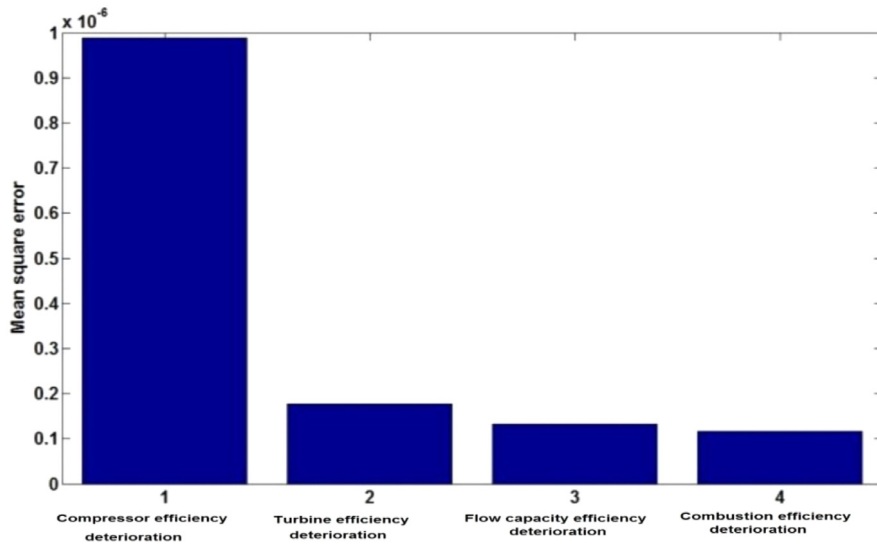


Fig. 14. MSE between engine model and degradation detection system (at Compressor pressure ratio = 0).

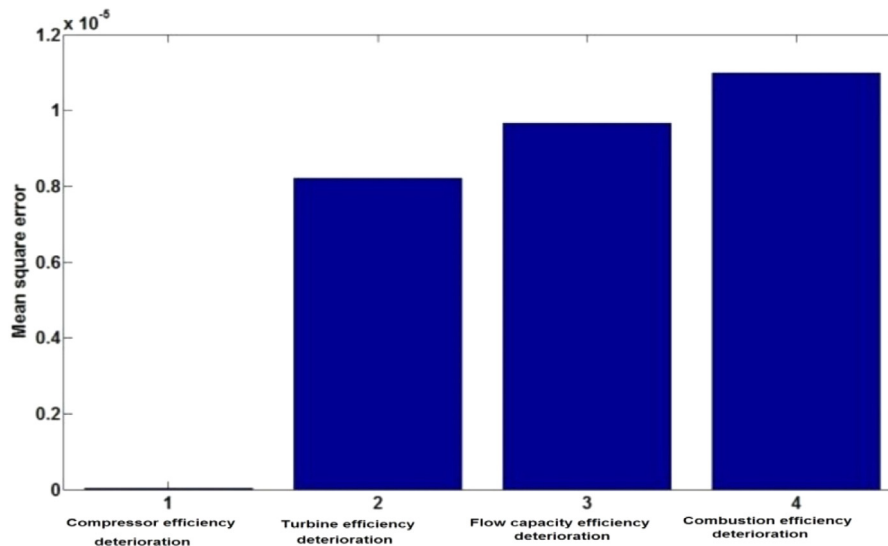


Fig. 15. MSE between engine model and degradation detection system (at Turbine inlet temperature = 0).

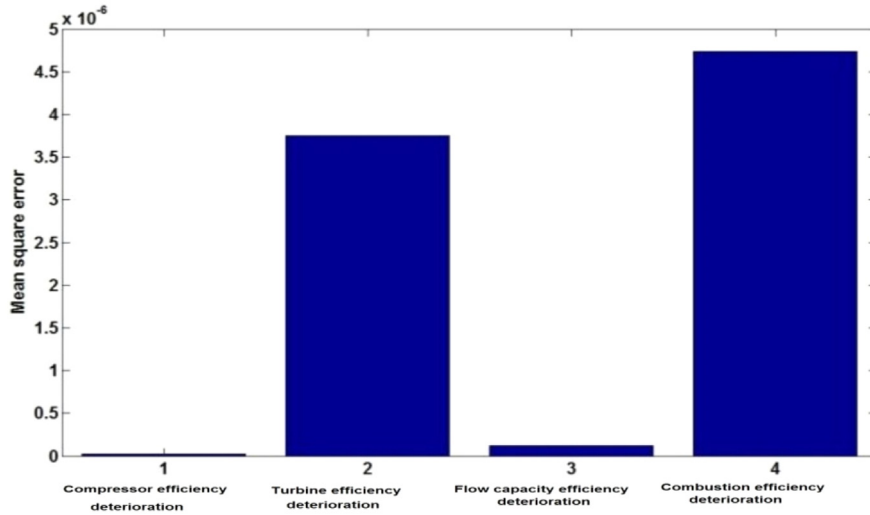


Fig. 16. MSE between engine model and degradation detection system (at Engine mass flow rate = 0).

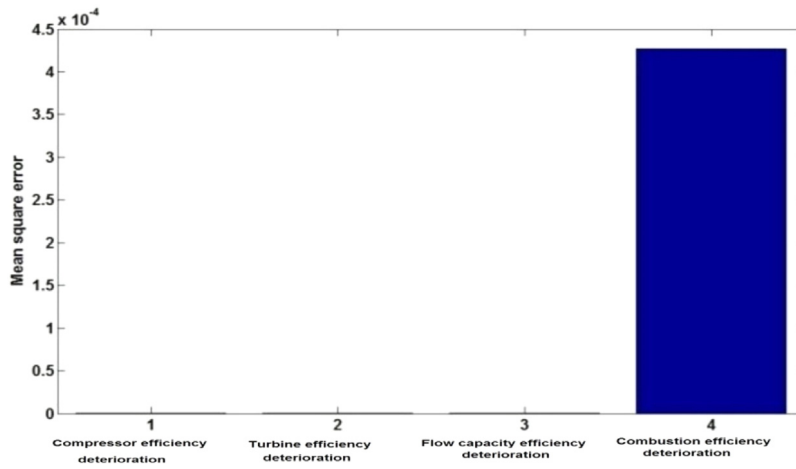


Fig. 17. MSE between engine model and degradation detection system (at Fuel mass flow rate = 0).

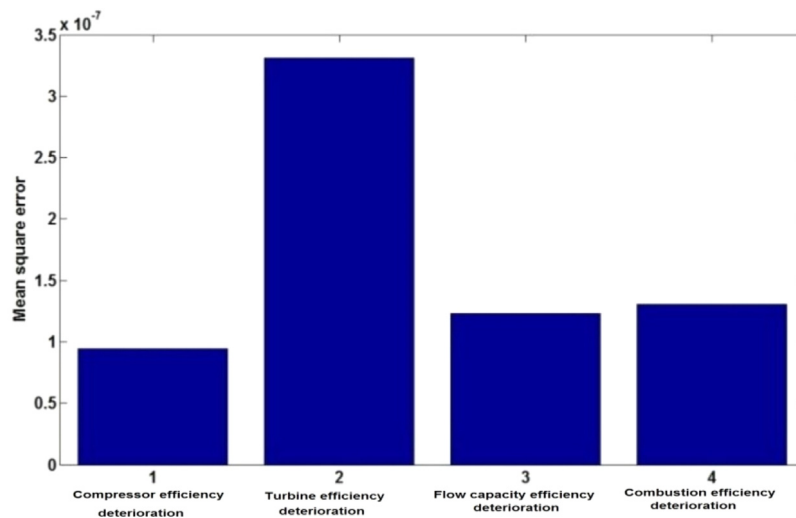


Fig. 18. MSE between engine model and degradation detection system (at Engine output load = 0).

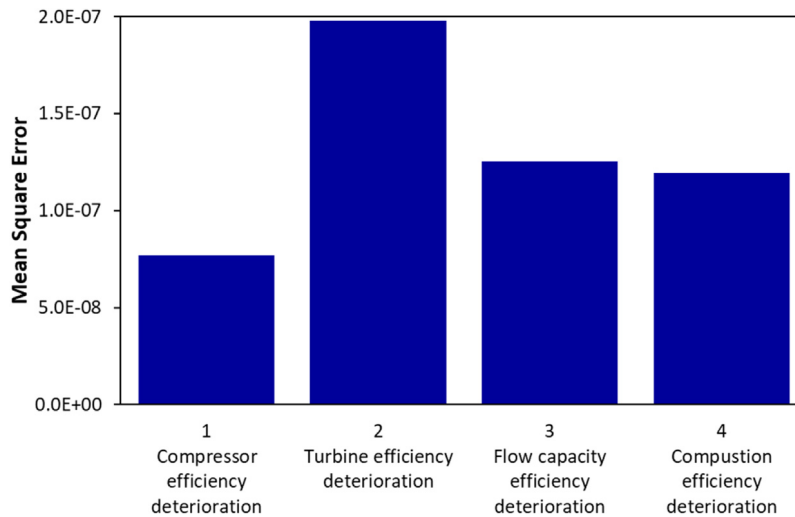


Fig. 19. The mean square errors between thermodynamic model and MFANN degradation detection model.

## 7. Results and discussion

### 7.1. Output load variation with different efficiency deterioration

Fig. 8 explains how the engine output load decreased with the increase of all component's efficiency deterioration levels.

### 7.2. Variation between thermodynamic model and MFANN

Fig. 9 illustrates the MSE between thermodynamic model and MFANN performance model (4788 training dataset); it was given the maximum MSE for seven output measurements about  $7.81 \times 10^{-7}$  in T6 (fuel mass flow rate).

Fig. 10 illustrates the MSE between thermodynamic model and the MFANN performance model (101 outside training dataset); it was given the maximum MSE for seven output measurements about  $6.91 \times 10^{-5}$  in T1 (Air inlet filter differential pressure). The second maximum MSE was determined from the engine output load.

### 7.3. Integrated degradation detected system testing result

Figs. 11 to 18 illustrate the performance of integrated degradation detected system when it was tried with testing data (101 outside training dataset) eight times, for each state the component degradation was calculated when one of measurements parameter was blocked and given irrational values such as zero value, which was the maximum MSE for all stats of component degradation factors about  $4 \times 10^{-4}$  in T4 (Combustion efficiency) at input 7 = 0.

Fig. 19 illustrates the MSE between the thermodynamic model and MFANN degradation detected system when it was tried with testing data (101 outside training dataset) for four output components degradation factor range about  $1.97 \times 10^{-7}$  in T<sub>2</sub> (Turbine efficiency state). However, the minimum MSE of  $9.34 \times 10^{-8}$  was achieved by compressor efficiency. Both MSE related to the engine capacity and the combustion efficiency were about  $1.3 \times 10^{-7}$ .

## Conclusion

The paper presents a model based on MFANN to develop the detection of industrial gas turbine degradation for improving energy efficiency and waste minimization. This is considered as a robust fault diagnosis system with an acceptable error margin. It is summarized as follows:

1. The simulation of the industrial gas turbine was investigated by using a thermodynamic principle and the utilization of alternative maps for the main engine components.
2. A review of the types of deterioration in industrial gas turbines as well as a survey of the concepts, types and construction phases of the MFANN model, achieved by:
  - Constructing a thermodynamic model to calculate the engine's performance
  - Constructing a MFANN model to calculate the engine's performance rapidly
  - Constructing a MFANN model for diagnosis of the engine's component degradation, and
  - Constructing an integrated degradation detection system to diagnose the engine's component degradation (estimated at 4788 cases) when there was damage in one of the measurement parameters.
3. Choosing the best structure for the MFANN model was decided based on trial-and-error, to obtain a minimum mean square error. In order to verify the proposed MFANN model, the model was tested against a set of data that was not used in the MFANN training. The result of this comparison was satisfactory giving a MSE of  $5 \times 10^{-3}$  maximum.
4. Training and testing of the MFANN was done with all training data (4788 case) with MSE about  $6 \times 10^{-4}$ .

## Declaration of competing interest

The authors declare that they have no known competing financial interests or personal relationships that could have appeared to influence the work reported in this paper.

## CRediT authorship contribution statement

**Adel Alblawi:** Formal analysis, Investigation, Methodology, Supervision.

## References

- Amirkhani, S., Chaibakhsh, A., Ghaffari, A., 2019. Nonlinear robust fault diagnosis of power plant gas turbine using Monte Carlo-based adaptive threshold approach. *ISA Trans.* <http://dx.doi.org/10.1016/j.isatra.2019.11.035>.
- Asgari, Chen, Xiao Qi, Menhaj, Mohammad B., Sainudiin, Raazesh, 2013. *Artificial Neural Network-Based System Identification for a Single-Shaft Gas Turbine*. ASME Paper No: GTP-13-1118.

- Bai, J., Liu, S., Wang, W., Chen, Y., 2019. Study on identification method for parameter uncertain model of aero gas turbine. *Propuls. Power Res.* <http://dx.doi.org/10.1016/j.jprr.2019.11.004>.
- Betocchi, R., Spina, P.R., Torella, G., 2002. Gas Turbine Health Indices Determination By using Neural Networks. ASME Paper.
- Cohen, H., Rogers, C.F.C., Saravanamuttoo, H.I.H., 1987. *Gas Turbine Theory*, third ed. Longman Scientific & Technical, Longman Group Limited, Essex, Great Britain.
- Farahat, M.A., Talaat, M., 2012. The using of curve fitting prediction optimized by genetic algorithms for short-term load forecasting. *Int. Rev. Electr. Eng.* 7 (6), 6209–6215.
- Gobran, M.H., 2013. Off-design performance of solar Centaur-40 gas turbine engine using Simulink. *Ain Shams Eng. J.* (2013), 4, 285–4, 298.
- Guasch, A., Quevedo, J., Milne, R., 2000. Fault diagnosis for gas turbines based on the control system. *Eng. Appl. Artif. Intell.* 13 (4), 477–484. [http://dx.doi.org/10.1016/S0952-1976\(00\)00014-2](http://dx.doi.org/10.1016/S0952-1976(00)00014-2).
- Hanachi, H., Liu, J., Kim, I.Y., Mechefske, C.K., 2019. Hybrid sequential fault estimation for multi-mode diagnosis of gas turbine engines. *Mech. Syst. Signal Process.* 115, 255–268. <http://dx.doi.org/10.1016/j.ymssp.2018.05.054>.
- Kazemi, H., Yazdizadeh, A., 2020. Fault detection and isolation of gas turbine engine using inversion-based and optimal state observers. *Eur. J. Control* <http://dx.doi.org/10.1016/j.ejcon.2020.01.002>.
- Lakshminarasimha, A.N., Boyce, M.P., Meher-Homji, C.B., 1994. Modeling and analysis of gas turbine performance deterioration ASME paper. *J. Eng. Gas Turbines Power* 116 (1), 46–52.
- Li, J., Ying, Y., 2020. Gas turbine gas path diagnosis under transient operating conditions: A steady state performance model based local optimization approach. *Appl. Therm. Eng.* 170, 115025. <http://dx.doi.org/10.1016/j.applthermaleng.2020.115025>.
- McBride, Bonnie J., Zehe, Michael J., Gordon, Sanford, 2002. Coefficients for Calculating Thermodynamic Properties of Individual Species. SA/TP–2002-211556.
- Norvaisis, Edward K., 1974. *Simulation of Triple-Spool Turbo Engine*. National Technical information service U. S. department of commerce 5285 Port Royal Road, Springfield Va. 22151.
- Tamuno-ojuemi Ogaji, Stephen Ogajiye, 2003. *Advanced Gas-Path Fault Diagnostics for Stationary Gas Turbines* (Doctoral thesis). Cranfield University.
- Ogbonnaya, E., 2011. Gas turbine performance optimization using compressor online water washing technique. *Engineering* 3 (5).
- Roumeliotis, I., 2010. Degradation Effects on Marine Gas Turbines. Paper ID: NCH-2010-C4, Nausivios Chora.
- Simani, S., Patton, R.J., 2008. Fault diagnosis of an industrial gas turbine prototype using a system identification approach. *Control Eng. Pract.* 16 (7), 769–786. <http://dx.doi.org/10.1016/j.conengprac.2007.08.009>.
- Syverud, Elisabet, 2007. *Axial Compressor Performance Deterioration and Recovery through Online Washing* Doctoral thesis. Norwegian University.
- Talaat, M., Alsayyari, A.S., Farahat, M.A., Said, T., 2019. Moth-flame algorithm for accurate simulation of a non-uniform electric field in the presence of dielectric barrier. In: *IEEE Access*, Vol. 7, pp. 3836–3847.
- Talaat, M., Farahat, M.A., Mansour, Noura, Hatata, A.Y., 2020. Load forecasting based on grasshopper optimization and a multilayer feed-forward neural network using regressive approach. *Energy* 196, 117087.
- Talaat, M., Gobran, M.H., Wasfi, M., 2018. A hybrid model of an artificial neural network with thermodynamic model for system diagnosis of electrical power plant gas turbine. *Eng. Appl. Artif. Intell.* 68, 222–235.
- Wong, P.K., Yang, Z., Vong, C.M., Zhong, J., 2014. Real-time fault diagnosis for gas turbine generator systems using extreme learning machine. *Neurocomputing* 128, 249–257. <http://dx.doi.org/10.1016/j.neucom.2013.03.059>.
- Zhong, S., Fu, S., Lin, L., 2019. A novel gas turbine fault diagnosis method based on transfer learning with CNN. *Measurement* 137, 435–453. <http://dx.doi.org/10.1016/j.measurement.2019.01.022>.
- Zhou, D., Wei, T., Huang, D., Li, Y., Zhang, H., 2020. A gas path fault diagnostic model of gas turbines based on changes of blade profiles. *Eng. Fail. Anal.* 109, 104377. <http://dx.doi.org/10.1016/j.engfailanal.2020.104377>.